Optics & Laser Technology 65 (2015) 164–174

Contents lists available at ScienceDirect

Optics & Laser Technology

journal homepage: www.elsevier.com/locate/optlastec

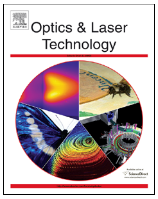

Laser cutting of lithium iron phosphate battery electrodes: Characterization of process efficiency and quality

Adrian H.A. Lutey [a,*], Alessandro Fortunato [a], Alessandro Ascari [a], Simone Carmignato [b], Claudio Leone [c]

[a] Università di Bologna, viale Risorgimento, 2, Bologna, Italy
[b] Università degli Studi di Padova, Stradella San Nicola, 3, Vicenza, Italy
[c] Università degli Studi di Napoli Federico II, Piazzale Tecchio, Napoli, Italy

ARTICLE INFO

Article history:
Received 26 May 2014
Received in revised form
15 July 2014
Accepted 28 July 2014
Available online 20 August 2014

Keywords:
Laser cutting
Battery electrodes
$LiFePO_4$

ABSTRACT

Lithium iron phosphate battery electrodes are subject to continuous-wave and pulsed laser irradiation with laser specifications systematically varied over twelve discrete parameter groups. Analysis of the resulting cuts and incisions with an optical profiler and scanning electron microscope gives insight into the dominant physical phenomena influencing laser cutting efficiency and quality. Measured incision depths are found to be piece-wise functions of average laser power, with the metallic conductor layers dominating the process due to their high thermal conductivity and low optical absorptance relative to the active coating layers. Cutting efficiency improves with shorter laser pulses and use of 532 nm radiation in place of 1064 nm. Complete electrode penetration takes place at lowest average power with pulse fluence in the ranges 35–40 J/cm^2 and 100–110 J/cm^2 for the cathode and anode, respectively, with 1064 nm beam wavelength. Per-pulse ablation depths are derived for the active coating layers under all tested conditions, giving new insight into the ablation behavior of each individual material. Defect size and coating layer delamination width are both found to be linked to cutting efficiency, with highest quality achieved for a given wavelength when overall cutting efficiency is optimized. Ideal parameters are found to be those maximizing the ablation efficiency of the metallic layers, as residual heat deposition in the films is minimized.

1. Introduction

Given appropriate infrastructure and environmental policy, proliferation of hybrid-electric vehicles (HEVs) and electric vehicles (EVs) in place of hydrocarbon-fueled variants may become a key to reduction in air pollution and carbon dioxide emissions in the transport industry [1,2]. Such a transition requires cheap, long service-life batteries with high energy density and specific energy. To this end, lithium batteries with olivine $LiFePO_4$ (LFP) cathodes [3] have recently seen much attention due to their high energy density [4], inherent safety [5–7], long service life [8,9], potentially low cost and good environmental compatibility [10–12]. Typically, LFP battery electrodes are 100–150 μm in thickness and consist of graphite coated copper anodes and LFP coated aluminum cathodes. During production, electrode films are cut to size and rolled or stacked consecutively, separated by porous films that allow the passage of electrolyte [13,14]. At present, repair and replacement of expensive tooling for the cutting phase of fabrication raises the cost of batteries, impacting the viability of automotive applications where large numbers of cells are required. In high volume battery production facilities, redundant cutting machines are further required to allow continuous operation during tool sharpening. Use of laser irradiation in place of mechanical cutting devices offers potential for quality improvements and cost reductions due to the contact free, low maintenance and flexible nature of the process. Application of laser technology in this field is relatively new with opportunity for growth, requiring knowledge of the factors and mechanisms influencing cut efficiency and quality. Recent studies have investigated laser cutting of lithium metal oxide (LMO) battery electrodes experimentally under specific conditions [14–17], achieving delamination and burr dimensions of less than 50 μm. Despite the relevance of LFP batteries and their emerging importance in the automotive industry, laser cutting of these electrode types has seen very limited discussion [18] and requires further investigation.

The physical phenomena at play during laser exposure have been studied at length for gas-free remote laser cutting and laser ablation of metals [19–21] and graphite [22]. In general, continuous-wave (CW) laser exposure leads to localized heating of the target and material removal via vaporization near the equilibrium boiling temperature [19,23]. In contrast, nanosecond pulsed laser exposure

---

[*] Corresponding author. Tel.: +39 0512093416; fax: +39 0512090484.
E-mail address: adrian.lutey2@unibo.it (A.H.A. Lutey).

http://dx.doi.org/10.1016/j.optlastec.2014.07.023
0030-3992/

with sufficiently high pulse fluence leads to superheating of the target surface well above the equilibrium boiling temperature [24]. Under these conditions, vaporization is governed by the Hertz–Knudsen relation [25,26] while liquid ejection may also take place above a discrete threshold fluence leading to a sharp increase in the ablation rate [27–30]. Nanosecond pulsed laser exposure of thin multi-layer films sees localized ablation take place under the focused beam during each laser pulse and vaporization or thermal degradation outside the exposed region on a much longer timescale due to thermal conduction between layers [31]. The use of nanosecond pulsed laser sources leads to higher cut quality than CW exposure due to a reduction in the heat affected zone (HAZ). Shorter pulses, in the picosecond and sub-picosecond ranges, may lead to nonlinear optical absorption, electron thermal diffusion and non-thermal stress fragmentation [32–34]; however, at present, cost considerations exclude laser sources in this range for high power industrial applications where longer pulses may suffice.

Previous investigations into laser cutting have compared individual high power CW and low power pulsed laser sources [14–18], with only the former capable of achieving cutting speeds appropriate for high volume battery production. Given the thermally sensitive nature of electrode active layers and the recent development of high power nanosecond pulsed fibre laser sources, a more thorough analysis of the factors affecting cutting efficiency and quality under pulsed conditions is necessary, taking into consideration the physical phenomena leading to material modification. The present work exhibits such an analysis, characterizing the response of LFP battery electrodes to laser irradiation over a far wider range of parameters than has previously been considered. Exposure velocity, laser operating mode, wavelength, pulse duration, repetition rate and pulse fluence have been systematically varied, with the total ablation depth and target surface characteristics measured with a 3D optical profiler and scanning electron microscope (SEM). To the authors' knowledge, no work has yet presented ablation rates for olivine LFP. Per-pulse ablation depths have therefore been calculated for the electrode active layers, giving new insight into the dominant factors influencing ablation of each individual material. Analysis of incisions achieved over the range of exposure conditions has allowed specification of optimum electrode cutting parameters in light of the physical phenomena influencing cutting efficiency and quality.

Table 1
Tested electrode layer compositions and thicknesses.

Film	Layer 1	Layer 2	Layer 3
Cathode	$LiFePO_4$ (45 μm)	Aluminum (20 μm)	$LiFePO_4$ (45 μm)
Anode	Graphite (47 μm)	Copper (10 μm)	Graphite (47 μm)

2. Experimental setup

2.1. Tested electrodes

Commercial LFP cathode and anode films were tested, with compositions and layer thicknesses as given in Table 1. For each film, the metallic layer and total electrode thicknesses were measured with a micrometer. The coating layer thicknesses were then calculated by assuming that both the upper and lower layers were of the same thickness. This assumption was then verified by SEM analysis of selected electrode sections. The amounts of binder material and other additives present in the coating layers was unknown.

2.2. Laser parameters and sample mounting

Five different laser sources, equipped with galvanometric scanners, were utilized for the experiments, yielding twelve discrete parameter groups. Table 2 presents the characteristics of each parameter group. Individual laser sources were utilized for groups 1–6, 7, 8, 9–10 and 11–12. The stability of all laser sources was guaranteed by the manufacturers as being $\geq 95\%$ over 5 h, while all beam profiles exhibited near-Gaussian spatial distributions. For each parameter group, the output power was controlled by adjusting the pump current from 20% to 100%, with all lasers stable over this range. The average beam power at the work piece was measured with a power meter for all parameter groups and pump current levels utilized in the experiments. Average beam power at 100% pump current for each parameter group is reported in Table 2.

A custom mounting was built to hold the samples horizontally under the focused beam via a series of holes and a vacuum source. Periodic cutouts were present to avoid contact between the sample and the mounting for at least 3 mm to either side of the exposed regions. These cutouts were not connected to the vacuum source so as to avoid deformation of the electrodes.

2.3. Procedure

Single line exposures of length 40 mm were executed on both electrodes at translational velocities of 100 mm/s, 500 mm/s and 1000 mm/s. For each velocity and test parameter group, the laser pump current was varied from 20% to 100% at intervals of 10%, yielding nine exposures for each combination. Each resulting incision was analyzed at ten different points with a 3D optical profiler operating in confocal mode [35], the characteristics of which are given in Table 3. Incision depth was taken as the difference between the lowest point in the exposed region and the average of several points in the flat regions immediately to either side of the exposure. For cases in which individual craters were present, incision depth was taken with reference to the

Table 2
Laser parameter groups under test conditions.

Parameter group	**1**	**2**	**3**	**4**	**5**	**6**	**7**	**8**	**9**	**10**	**11**	**12**
Wavelength (nm)	1064	1064	1064	1064	1064	1064	1064	1064	532	532	532	532
Operating mode[a]	P	P	P	P	P	P	P	CW	P	P	P	P
Pulse duration (ns)	4	30	30	200	200	200	120	–	4.5	4.2	1.4	1.4
Repetition rate (kHz)	500	500	100	500	100	20	100	–	20	10	500	100
Beam quality (M^2)	1.5	1.5	1.5	1.5	1.5	1.5	2	1.05	2	2	1.2	1.2
Spot diameter (μm)	25	25	25	25	25	25	54	46	27	27	16	16
Rayleigh range (μm)	320	320	320	320	320	320	1080	1460	540	540	325	325
Max. average power[b] (W)	19	19.2	18.8	19.1	18.8	18.7	84.8	315	4.3	2.8	8.2	1.6
Max. pulse energy[b] (μJ)	38	38	188	38	188	935	848	–	215	280	16	16
Max. fluence[b] ($J\ cm^{-2}$)	15	15	74	15	74	369	74	–	75	97	16	16

[a] P, pulsed; CW, continuous wave.

[b] Values at sample surface.